Reports

X-ray Diffraction to 302 Gigapascals: High-Pressure Crystal Structure of Cesium Iodide

H. K. Mao, Y. Wu, R. J. Hemley, L. C. Chen, J. F. Shu,
L. W. Finger

X-ray diffraction measurements have been carried out on cesium iodide (CsI) to 302 gigapascals with a platinum pressure standard. The results indicate that above 200 gigapascals CsI at 300 K has a hexagonal close-packed crystal structure with the ideal *c/a* ratio of 1.63 ± 0.01. The crystal structure and pressure-volume relations converge at high pressure with those of solid xenon, which is isoelectronic with CsI. The results indicate a significant loss of ionic bonding in the hexagonal close-packed metallic phase of CsI at ultrahigh pressure.

THE PHYSICS OF CONDENSED MATTER at ultrahigh pressures is of considerable current interest. In the past 15 years, the development of the diamond-anvil cell has steadily extended the maximum attainable static pressures from 50 to 550 GPa (*1*). Recently, evidence for metallization of hydrogen by band overlap has been reported above 200 GPa (*2*). The pressure measurements in most ultrahigh pressure experiments, however, were based on the extrapolation of the ruby fluorescence scale that was calibrated with a primary x-ray diffraction scale of Cu, Mo, Pd, and Ag to 100 GPa and Au and Cu to 180 GPa. With the development of energy-dispersive x-ray diffraction with synchrotron radiation (*3, 4*), diffraction measurements at higher pressures are now possible. A maximum pressure of 245 GPa has been obtained on x-ray diffraction of Re and 255 GPa on Fe (*5*). For an accurate pressure calibration, a material with much lower strength and a better defined isothermal equation of state than that of Re is essential. We report here x-ray diffraction results for CsI to an extended pressure range of 302 GPa. Platinum was used as an internal pressure calibrant. The equation of state of Pt has been studied extensively by shock-wave and theoretical techniques up to 660 GPa (*6*). Because of their low strength, CsI and Pt provide a more quasi-hydrostatic pressure environment than other materials studied previously by x-ray diffraction at ultrahigh pressures.

The behavior of CsI at high pressure has been used as a prototype for understanding crystal structures, equations of state, and metallization of materials at high pressures. For several years, this material has been the subject of intensive experimental (*3, 7–12*) and theoretical (*11, 13*) investigations. The ionic solid CsI is isoelectronic with the rare-gas solid Xe. With increasing pressure the interatomic forces in the ionic solid will begin to be dominated by short-range repulsive rather than long-range electrostatic terms. At sufficiently high compressions, the crystal structure and equation of state of CsI and Xe are therefore predicted to converge. Such a convergence, however, has never been confirmed experimentally in CsI and Xe (*9*) or any other material. In fact, xenon has been shown to transform from a cubic close-packed (ccp) to a hexagonal close-packed (hcp) structure with an intermediate mixed close-packed polytype phase (*14*), whereas CsI is reported to undergo a cubic-tetragonal-orthorhombic transition sequence (7) in which the highest pressure phase is not close-packed.

All previous x-ray diffraction studies of CsI were limited to maximum pressures of 95 GPa. In this pressure range, the crystal structures of CsI and Xe are complicated by transitions to intermediate phases. At higher compressions, with the increase in repulsive forces, a final configuration for CsI approaching Xe could be reached. In the present study, we have extended the pressure limit of previous studies of structural phase transitions and equations of state of CsI threefold to 302 GPa. In so doing, we have achieved a compression on this material that far exceeds that associated with the experimentally determined transition at 110 GPa from ionic to metallic bonding (*9*). The results are compared with recent x-ray diffraction measurements on Xe above 100 GPa (*14, 15*).

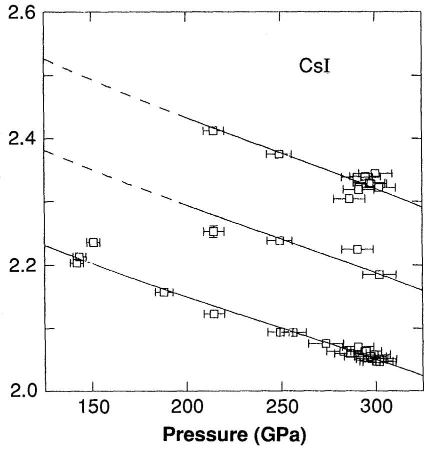

Fig. 1. Interplanar spacings for CsI at ultrahigh pressures. The error bars represent the standard deviation of pressures determined from the 111 and 200 diffraction peaks of the Pt standard. Between 150 and 200 GPa, only rapid, reconnaissance x-ray diffraction patterns (less than 10 min) were measured, and only the most intense peak of the triplet was fitted and plotted. The lines indicate the results calculated from an equation-of-state fit to the pressure-volume data above 200 GPa for the ideal hcp structure (*c/a* = 1.633).

A powdered mixture of CsI (99.999%) and Pt (99.999%), confined in a 40-μm hole of a T-301 stainless steel gasket, was loaded into a diamond-anvil cell with beveled diamonds (*16*). Data were obtained at the National Synchrotron Light Source by energy-dispersive x-ray diffraction techniques with polychromatic (white) x-radiation (*3, 4*). The primary beam was collimated to 10 μm by two sets of slits, so that any pressure variation within the sample could be determined and diffraction from the gasket could be avoided completely. The diffracted beam was collected at an angle of 20.0° with a collimator system for high spatial resolution and a solid-state Ge detector for energy resolution. Polycrystalline diffraction patterns included 111 and 200 lines of Pt and three CsI lines. Pressure was determined on the basis of the new Pt pressure scale (*6*).

At pressures above 200 GPa, the diffraction pattern of CsI displays a triplet of peaks that is identical to the 100, 002, and 101 triplet of hcp Xe above 100 GPa and is typical of an ideal hcp metal. The triplet also falls on the extrapolation of the 011, 101, and 110 triplet of the CsI phase above 60 GPa previously assigned as orthorhombic distortion of the B2 structure (*7, 17*). An hcp-like structure is the preferred assignment for the high-pressure phase above 200 GPa, however, as indicated by the repre-

---

H. K. Mao, R. J. Hemley, L. C. Chen, J. F. Shu, L. W. Finger, Geophysical Laboratory, Carnegie Institution of Washington, 2801 Upton Street, NW, Washington, DC 20008.
Y. Wu, Center for X-ray Optics, Lawrence Berkeley Laboratory, Berkeley, CA 94720.

Table 1. X-ray diffraction data for CsI at 249 ± 7 GPa and Xe at 137 ± 1 GPa (*14*). Since pressures are different for the two sets of data, it is instructive to compare the relative *d*-spacings and intensities (*I*), not their absolute values. The strongest diffraction line in each set is given a relative intensity value of 100.

CsI		Xe		Ideal hcp		Orthorhombic	
d_{obs} (Å)	I_{obs}	d_{obs} (Å)	I_{obs}	*hkl*	I_{calc}	*hkl*	I_{calc}
2.375	18	2.504	20	(100)	22	(011)	100
2.239	22	2.382	28	(002)	26	(101)	100
2.094	100	2.246	100	(101)	100	(110)	100

sentative diffraction data for CsI and Xe at high pressure in Table 1. The observed and calculated intensities for the hcp assignment are in good agreement. In contrast, the calculated intensities of the orthorhombic cell do not match the observed values. One has to resort to preferred orientation in the diamond cell to explain the total intensity mismatch. Finally, there is a close similarity between the diffraction pattern of CsI at high pressure and the hcp phase of Xe (*14*).

The high-pressure phase of CsI documented here is stable to at least 302 GPa. The pressure dependence of the diffraction peaks in the high-pressure region is shown in Fig. 1. Although the *d*-spacing of each diffraction line changed continuously over this pressure range, the ratios of *d*-spacings of different lines remained strikingly constant. Such constancy suggests constraints by symmetry or structure. The *c*/*a* ratio calculated from the three diffraction lines is 1.63 with a standard deviation of ±0.01 among data points above 200 GPa. The ratios are in excellent agreement with the hcp constraints of hexagonal symmetry and of close-packed spherical atoms with an ideal *c*/*a* ratio of 1.633. On the other hand, the B2 structure with the type of orthorhombic distortion specified in the previous investigations does not have an intrinsic geometrical or potential limit to constrain the axial ratio. The ordering of Cs^+ and I^- ions and the effect of residual, long-range, electrostatic interactions could cause minor distortion of the hcp lattice. The distortion, however, is not detected with the resolution of the present study (Fig. 1).

The hcp assignment results in a molar volume 10% smaller than the volume based on the orthorhombic assignment. The experimentally determined volumes for CsI as a function of pressure up to 302 GPa are plotted in Fig. 2. At the highest pressures (302 ± 8 GPa) the compression V/V_0 is 0.28. This value is well below the critical compression for metallization calculated by band-structure methods (*12*) and observed experimentally (*9*) ($V/V_0 \sim 0.43$ to 0.50). The recent x-ray diffraction data for Xe determined by Jephcoat *et al.* (*14*) and Reichlin *et al.* (*15*) to 137 and 172 GPa, respectively, are also compared in Fig. 2. The CsI and Xe volumes are indistinguishable where the comparison can be made. No theoretical calculations have yet been reported for close-packed CsI (or for CsI in any structure at the very high pressures reached in our experiments). We compare the results of a 300 K equation of state calculated from the exp-6 potential fit to the augmented-plane-wave (APW) calculations for CsI up to 100 GPa (*11*); the hcp structure was assumed for comparison with the x-ray data above 100 GPa. At the highest pressures the volumes calculated from this equation of state are significantly higher than those determined from the x-ray data. This result may indicate that changes in electronic properties with pressure tend to soften the repulsive ionic interactions, consistent with increasing metallic character of CsI above 110 GPa. We also compare the equation of state calculated for close-packed Xe to 150 GPa, using APW methods (*18*). This curve closely tracks the present results for CsI in addition to the existing experimental data for Xe, again demonstrating the isomorphism between the two materials at high pressures. Further theoretical calculations are required to compare the electronic structure of the high-pressure hcp metallic phases of CsI and Xe.

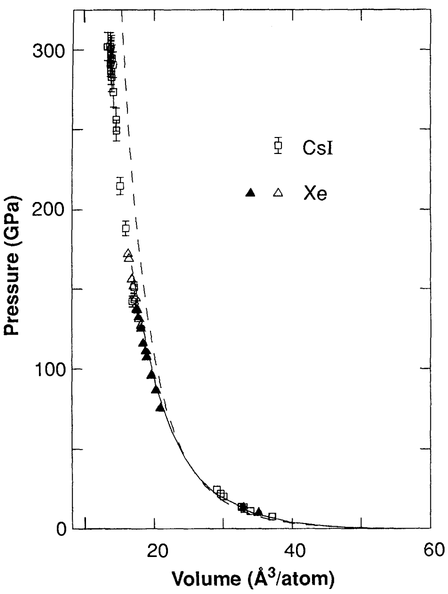

Fig. 2. Pressure-volume data for CsI and Xe to ultrahigh pressure: CsI, squares (this work); Xe, filled triangles (*14*) and open triangles (*15*). The dashed line is the room-temperature equation of state for CsI in the hcp structure calculated on the basis of the pure exp-6 potential determined in (*11*). The solid line is the static-lattice curve calculated with APW methods for Xe (*18*). The latter calculation was carried out for the ccp [or face-centered cubic (fcc)] structure; the difference in calculated equation of state for ccp and hcp is negligible on this scale.

REFERENCES AND NOTES

1. G. J. Piermarini and S. Block, *Rev. Sci. Instrum.* **46**, 973 (1975); P. M. Bell and H. K. Mao, *Carnegie Inst. Washington Yearb.* **74**, 399 (1975); H. K. Mao and P. M. Bell, *Science* **191**, 851 (1976); *ibid.* **200**, 1145 (1978); P. M. Bell, H. K. Mao, K. Goettel, *ibid.* **226**, 542 (1984); J. A. Xu, H. K. Mao, P. M. Bell, *ibid.* **232**, 1404 (1986).
2. H. K. Mao and R. J. Hemley, *Science* **244**, 1462 (1989).
3. Y. K. Vohra, K. E. Brister, S. T. Weir, S. J. Duclos, A. L. Ruoff, *ibid.* **231**, 1136 (1986).
4. A. P. Jephcoat *et al.*, *Natl. Synchrotron Light Source Annu. Rep.* **1986**, 323 (1986).
5. Y. K. Vohra, S. J. Duclos, K. E. Brister, A. L. Ruoff, *Phys. Rev. Lett.* **61**, 574 (1988).
6. N. C. Holmes, J. A. Moriarty, G. R. Gathers, W. J. Nellis, *J. Appl. Phys.* **66**, 2962 (1989). The 300 K equation of state determined for Pt in this study has the form: pressure P = 798.31 GPa $[(1 - X)/X^2]e^{7.2119(1-X)}$, where $X = a/a_0$ is the ratio of the lattice parameter of Pt at high pressure to that at zero pressure.
7. K. Asaumi, *Phys. Rev. B* **29**, 1118 (1984); T.-L. Huang and A. L. Ruoff, *ibid.*, p. 1112; E. Knittle and R. Jeanloz, *Science* **223**, 53 (1984); *J. Phys. Chem. Solids* **46**, 1179 (1985).
8. I. N. Makarenko, A. F. Goncharov, S. M. Stishov, *Phys. Rev. B* **29**, 6018 (1984); J. P. Itie, A. Polian, J. M. Besson, *ibid.* **30**, 2309 (1984); Y. K. Vohra, S. T. Weir, K. E. Brister, A. L. Ruoff, *Phys. Rev. Lett.* **55**, 977 (1985); Q. Williams and R. Jeanloz, *ibid.* **56**, 163 (1986); *ibid.* **59**, 1132 (1987).
9. A. N. Zisman, I. V. Aleksandrov, S. M. Stishov, *Phys. Rev. B* **32**, 484 (1985). Zisman *et al.* concluded that the volumes of Xe and CsI coincided above 15 GPa. However, there is a significant unresolved difference between the equations of state of CsI determined from their diffraction data and that calculated from other static experiments (*3*, *7*). Zisman *et al.* indexed Xe as the cubic-close-packed (ccp) structure and CsI as the tetragonally distorted B2 structure; the latter is a more open structure than ccp. A similar unit-cell volume for the two actually implies that the nearest-neighbor distance in CsI is considerably shorter than that of Xe. In addition, Xe was later found to transform to a complex close-packed structure above 17 GPa (*14*). Thus these results cannot be used as evidence that Xe and CsI approached the same structure and density.
10. R. Reichlin, M. Ross, S. Martin, K. A. Goettel, *Phys. Rev. Lett.* **56**, 2858 (1986).
11. H. B. Radousky, M. Ross, A. C. Mitchell, W. J. Nellis, *Phys. Rev. B* **31**, 1457 (1985); M. Ross and F. J. Rogers, *ibid.*, p. 1463.
12. C. A. Swenson, J. W. Shaner, J. M. Brown, *ibid.* **34**, 7924 (1986).
13. J. Aidun, S. T. Bukowinski, M. Ross, *ibid.* **29**, 2611 (1984); S. Satpathy, N. E. Christensen, O. Jepsen, *ibid.* **32**, 6793 (1985).
14. A. P. Jephcoat *et al.*, *Phys. Rev. Lett.* **59**, 2670 (1987).
15. R. Reichlin *et al.*, *ibid.* **62**, 669 (1989).
16. A. P. Jephcoat, H. K. Mao, P. M. Bell, in *Hydrothermal Experimental Techniques*, G. C. Ulmer and H. L. Barnes, Eds. (Wiley-Interscience, New York, 1987),

p. 469; H. K. Mao, in *Simple Molecular Systems at Very High Density*, P. Loubeyre, A. Polian, N. Boccara, Eds. (Plenum, New York, 1989), p. 221.
17. An analysis of the structure of CsI below 200 GPa, including the mechanism of the transformation from B2 to the hcp-like structure, will be presented elsewhere (H. K. Mao *et al.*, in preparation).
18. M. Ross and A. K. McMahan, *Phys. Rev. B* **21**, 1658 (1980).
19. We acknowledge the invaluable assistance of D. E. Cox at beamline X-7A of the National Synchrotron Light Source, Brookhaven National Laboratory. We thank N. C. Holmes, J. A. Moriarty, G. R. Gathers, and W. J. Nellis for providing information on the Pt equation of state. We also thank Q. Williams, R. Reichlin, and A. L. Ruoff for constructive comments on the manuscript. Supported by the National Science Foundation under grants EAR-8610068, EAR-8708127, EAR-8720326, and EAR-8817263 by the Carnegie Institution of Washington.

10 July 1989; accepted 22 September 1989

Protein Crystal Growth in Microgravity

LAWRENCE J. DELUCAS, CRAIG D. SMITH, H. WILSON SMITH,
SENADHI VIJAY-KUMAR, SHOBHA E. SENADHI, STEVEN E. EALICK,
DANIEL C. CARTER, ROBERT S. SNYDER, PATRICIA C. WEBER,
F. RAYMOND SALEMME, D. H. OHLENDORF, H. M. EINSPAHR,
L. L. CLANCY, MANUEL A. NAVIA, BRIAN M. MCKEEVER,
T. L. NAGABHUSHAN, GEORGE NELSON, A. MCPHERSON,
S. KOSZELAK, G. TAYLOR, D. STAMMERS, K. POWELL,
G. DARBY, CHARLES E. BUGG

The crystals of most proteins or other biological macromolecules are poorly ordered and diffract to lower resolutions than those observed for most crystals of simple organic and inorganic compounds. Crystallization in the microgravity environment of space may improve crystal quality by eliminating convection effects near growing crystal surfaces. A series of 11 different protein crystal growth experiments was performed on U.S. space shuttle flight STS-26 in September 1988. The microgravity-grown crystals of γ-interferon D^1, porcine elastase, and isocitrate lyase are larger, display more uniform morphologies, and yield diffraction data to significantly higher resolutions than the best crystals of these proteins grown on Earth.

PROTEIN CRYSTALLOGRAPHY REquires crystals of suitable size and quality for high-resolution diffraction analyses. A new development in protein crystal growth involves studies of crystal growth processes in the microgravity environment obtainable in space (*1, 2*). The major motivation behind these space experiments is to eliminate the density-driven convective flow that accompanies crystal growth in gravitational fields (*3, 4*). In addition, sedimentation of growing crystals, which can interfere with the formation of single crystals, is eliminated in the absence of gravity.

Microgravity protein crystal growth experiments performed on Spacelab 1 by Littke and John (*5*) indicated that the space-grown crystals from a liquid-liquid diffusion system were larger than crystals obtained by the same experimental system on Earth. Experiments on four U.S. space shuttle missions in 1985 and 1986 led to development of an apparatus for protein crystal growth by vapor diffusion techniques (*6*). We used this equipment for a series of protein crystal growth experiments on U.S. space shuttle flight STS-26 in September 1988. The results of these experiments are presented.

The vapor diffusion technique used on STS-26 is closely related to the hanging drop method (*7*), and thus the microgravity results can be compared with extensive data obtained from experiments on Earth. The hardware was adapted from that used on a series of four shuttle missions in 1985 and 1986 (*6*). Crystals were grown in 40-µl droplets that were extruded from syringes and subsequently permitted to equilibrate with solutions of precipitating agents contained within closed chambers. Each experiment was performed within a chamber (5.3 cm^3) with clear plastic windows. Before the launch, a double-barreled syringe was loaded with protein solution and crystallizing (precipitating) solutions in adjacent barrels. The mouths of these double-barreled syringes were stoppered during launch and landing. The chamber contained an absorbent material that was saturated with a solution of the precipitating agent. All solutions were loaded ~24 hours before the launch. Once in orbit, crystal growth was activated by extruding the solutions onto the tip of the syringe, where mixing of the protein solution and precipitating agent was achieved by repeatedly withdrawing and extruding the solutions. The suspended droplet was then allowed to equilibrate with the surrounding solution of precipitating agent. The protein droplets were photographed after activation and at 24-hour intervals during the 3-day experiments. After 3 days, the solutions and suspended crystals were withdrawn into the syringes and stoppered for return to Earth (*8*).

Control experiments on Earth were performed in equipment identical to that used for the shuttle experiments. The control experiments were begun 7 days after the shuttle landed; the same protein solutions and identical loading, activation, and deactivation times were used in the control experiments as in the STS-26 experiments. Extensive control experiments were also performed in prototypes of the space shuttle hardware before and after the shuttle experiments were completed.

X-ray diffraction photographs were used for qualitative evaluation of diffraction resolutions. The results from these analyses are consistent with the more detailed studies of three-dimensional (3-D) data sets measured with the area detector systems (*9*). Because evaluation of diffraction resolutions from photographs is highly subjective, and is often dependent on crystal orientations, we have depended primarily on 3-D intensity data sets for comparison of space- and Earth-grown crystals.

Intensity data sets from crystals of three proteins were analyzed in a variety of different ways (Fig. 1). The largest Bragg angles at which usable data could be measured were assembled, and the percentage of data above background levels throughout the data collection range was evaluated. Plots were made of average $I/\sigma(I)$ values, where I is intensity, versus diffraction resolution and of percentages of data above various cutoff levels as functions of resolution. Data sets from space- and Earth-grown crystals were compared by using Wilson plots (*10*). The Wilson plot can be used to estimate the

---

L. J. DeLucas, C. D. Smith, H. W. Smith, S. Vijay-Kumar, S. E. Senadhi, S. E. Ealick, C. E. Bugg, University of Alabama at Birmingham, Center for Macromolecular Crystallography, Birmingham, AL 35294.
D. C. Carter and R. S. Snyder, George Marshall Space Flight Center, Huntsville, AL 35812.
P. C. Weber, F. R. Salemme, D. H. Ohlendorf, E. I. du Pont de Nemours & Company, Central Research and Development Department, Wilmington, DE 19880.
H. M. Einspahr and L. L. Clancy, Upjohn Company, Kalamazoo, MI 49001.
M. A. Navia and B. M. McKeever, Merck Sharp & Dohme Research Laboratories, Rahway, NJ 07065.
T. L. Nagabhushan, Schering-Plough Corporation, Bloomfield, NJ 07003.
G. Nelson, Astronomy Department, University of Washington, Seattle, WA 98195.
A. McPherson and S. Koszelak, University of California at Riverside, Riverside, CA 92521.
G. Taylor, Laboratory of Molecular Biophysics, University of Oxford, Oxford OX1 3QU, United Kingdom.
D. Stammers, K. Powell, G. Darby, Wellcome Research Laboratories, Beckenham BR3 3BS, United Kingdom.